Fusion Engineering and Design 181 (2022) 113214

Contents lists available at ScienceDirect

Fusion Engineering and Design

journal homepage: www.elsevier.com/locate/fusengdes

Development of flexible filler ribbons by melt spinning for joining W to CuCrZr material for heat sink application

I. Izaguirre [a,*], J. de Prado [a], M. Sánchez [a], D. Salazar [b], A. Ureña [a]

[a] Materials Science and Engineering Area, ESCET, Rey Juan Carlos University, C/Tulipán s/n, Móstoles, Madrid 28933, Spain
[b] BCMaterials - Basque Center Centre for Materials, Applications and Nanostructures, UPV/EHU Science Park, Leioa 48940, Spain

ARTICLE INFO

Keywords:
Brazing
Fusion reactor
Tungsten
Flexible filler
Melt-spun ribbons

ABSTRACT

This paper studies the use of the melt-spinning technique as an alternative filler fabrication route to obtain flexible 80Cu-20Ti ribbons, which presents flexible and adaptability properties to cover the divertor or first wall pipe in future fusion reactors. The results showed that best conditions are achieved using a 0.8 mm diameter of the nozzle and 30 m/s of the linear wheel-speed. This condition allows to change the microstructure of the fabricated ribbons giving rise to a lower Cu_4Ti intermetallic phase formation enhancing the adaptability properties. Ribbon dimensions are high enough to cover the perimeter of the pipe. Best conditions were selected to use as filler material in W-CuCrZr brazed joints at 960 °C. The results showed the consecution of high metallic continuity interfaces. Besides, the selected brazing conditions did not cause any thermal effect in the W base material but caused a softening effect in the CuCrZr base material as a consequence of the coarsening process of the hardening precipitates.

1. Introduction

The development of the future DEMO fusion reactor is associated with the development of materials and manufacturing techniques to their application in the First Wall (FW) or Plasma Facing Materials (PFM). Several authors have demonstrated, during the last few years, that tungsten is the most promising material to face the plasma due to its appropriate thermomechanical properties for the selected application [1,2]. The extracted heat from the plasma must be conducted to a heat sink component through the tungsten layer or monoblock. According to the current divertor water coolant design, this component will be made of CuCrZr alloy pipes that cooled the tungsten plasma facing monoblocks [3]. Therefore, a reliable joint between both materials must be achieved. The solution must overcome some difficulties such as relieves the thermal stress during operation caused by the different Coefficient of Thermal Expansion (CTE) of both base materials [4,5]. Besides, the difficult geometry of the joint, a square profile tungsten monoblock join to a round pipe, makes the process even more difficult.

Brazing, as joining manufacturing process, is a reliable technique that uses lower joining temperatures than the base material melting points [6] or shorter times concerning solid-state ones [7]; therefore, it has high applicability for industrial production. Besides, it allows performing post-weld heat treatment in the whole component inside the furnace. This technique has been previously explored by many authors to join W-CuCrZr for this application. For example, Mou et al. [8] used pure copper to prepared mock-ups to evaluate their response under high heat flux test, Singh et al. [9] used vacuum brazing to join both materials with NiCuMn filler and Peng et al. [10] brazed W-CuCrZr with Cu-22TiH_2. However, most of the conventional fillers have elements forbidden in terms of neutron activation or do not exhibit flexible capabilities in ribbon form [11,12].

In this study, manufacturing process of Cu-20Ti alloy by melt-spinning technique to fabricated flexible filler ribbons for its application in W-CuCrZr joints is carried out. This joint will conform part of the divertor component in the DEMO reactor. By adding titanium to copper, a reduction of the melting range is achieve and, therefore, the as-receive properties of the parents material are better preserved in terms of thermal affectation [13].

This filler composition has already been shown to be suitable for the above mentioned application showing the consecution of high strength and continuous joints [14]. However, the ribbons used, obtained from a solidified drop of the alloy, do not meet the flexible criteria. The proposed manufacturing process ejects the melted alloy into a rotatory copper wheel giving rise to high cooling rates of approximately 10^6 K/s,

* Corresponding author.
E-mail address: ignacio.izaguirre@urjc.es (I. Izaguirre).

https://doi.org/10.1016/j.fusengdes.2022.113214
Received 10 January 2022; Received in revised form 22 June 2022; Accepted 23 June 2022
Available online 29 June 2022

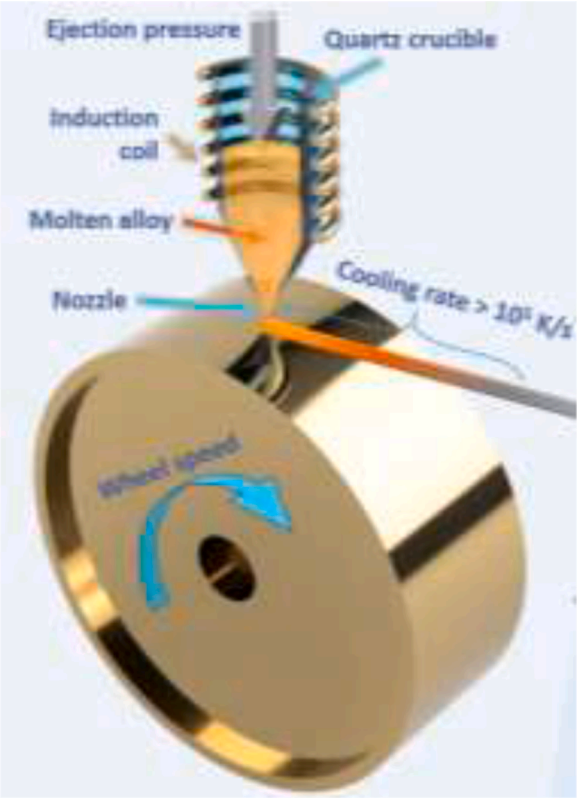

Fig. 1. Scheme of melt spinning technique [20].

depending on the specific parameters used. This solidification process avoids diffusion phenomena inhibiting partially or totally the formation of intermetallic compounds. Therefore, it provides filler tapes with sufficient flexibility and adaptability properties to cover the mentioned components. In addition, under certain conditions the process allows the formation of an amorphous structure, which, unlike crystalline structures, confers the desired flexibility. Moreover, it allows eliminating the organic binder necessary to achieve flexibility when the filler is obtained by other techniques [7], which could affect the filler composition due to the binder decomposition with temperature.

The proposed technique, melt-spinning, was previously used for this objective by Yuxin Xu et.al [15] using a different Cu-Ti alloy to join a supper alloy to tungsten obtaining amorphous materials and high-quality joints. Furthermore, the consecution of different amorphous filler compositions had been reported by this technique in other systems, $SmFe_{12}$ by Tamura et al. [16], $Nd_2Fe_{14}B$ by Salazar et al. [17], and $Fe_{67}Y_{33}$ by Bouhbou et al.[18].

The aim of this paper is both to study the feasibility of the manufacturing process to obtain flexible ribbons fillers and determine the brazeability of W-CuCrZr joints by using Cu-Ti filler material processed by melt-spinning.

2. Experimental details

2.1. Materials and fabrication of flexible filler ribbons

The master alloy used for the fabrication of the fillers by melt-spinning technique was obtained from a solidified drop of the alloy. By that, pure copper and titanium powders with 80Cu20Ti composition supplied by *Cymit Química,* copper powders, -325 mesh, +325 mesh, > 99% purity and titanium powders, -200 mesh, 99.5%, were compacted applying 750 MPa for 2 min to produce pellets of 13 mm of diameter. The device used to make the pellets was a hydraulic press supplied by Unicraft WPP 50 E. The pellets were molten at 1110 °C (100 °C above the melting point of the alloy [19]) for 1 h in a high vacuum furnace, that allows working under vacuum with a residual pressure of 10^{-6} mbar, obtaining small ingots of the master alloy.

Table 1
Fabrication parameters of filler ribbons by melt spinning technique. D is the internal diameter of the nozzle and v the linear speed of the copper wheel.

Cond	D (mm)	v (m/s)
C1	**1**	**35**
C2	**0.95**	**44**
C3	**0.9**	**30**
C4	**0.9**	**35**
C5	**0.8**	**30**

Melt-spun ribbons of 80Cu-20Ti alloy were obtained by melt-spinning technique. A schematic representation of this technique is shown in Fig. 1, where parameters as nozzle size, ejecting pressure, wheel-speed, temperature of the molten alloy and the distance between the nozzle and the copper wheel control the fabrication process. In this work, five different conditions of nozzle and wheel-speed were tested and evaluated for their application as filler materials modifying the diameter of the nozzle and the linear wheel-speed as shown in Table 1 [21]. All parameters control the nominal cooling rate of the alloy by controlling the quantity of material ejected and the wheel-speed. Therefore, it has influence in the microstructure and physical/mechanical properties of the fabricated ribbons.

Finally, brazing of tungsten and CuCrZr alloy were performed using the fabricated filler. Tungsten base material was supplied by Plansee in hot rolled plate form condition. The final thickness of the process is 5 mm. According to the manufacturer it has a purity of 99.99 % and recrystallized microstructure as a consequence of the rolling process. CuCrZr alloy supplied by *KME* with the following composition according X-Ray Fluorescence (XRF) on the CuCrZr base material: 98,9% Cu ± 0,09%, 0,773% Cr ± 0,01% and 0,0728% Zr ± 0,001% correspondingly in EN (European Norms) standards and in UNS (Unified Numbering System).

2.2. Brazing process

A high vacuum furnace was used for the brazing tests at a residual pressure of 10^{-6} mbar. Before the brazing tests, the exposed surface of both base materials was polished with 4000 grid silicon carbide paper. In the case of tungsten samples, rolling direction was placed perpendicular to the joint interface.

Brazing of all specimens was performed at 960 °C, holding that temperature for 10 min. Heating and cooling rates were 5 °C/min. Brazing parameters were chosen according to previous studies of the group where brazing conditions of Cu-Ti filler were optimized [13].

2.3. Characterization techniques

Flexibility and adaptability tests were carried out to determine those properties in the melt-spun ribbons. By that, ribbons were placed over the surface of the divertor or first wall simulating pipe of 20 mm diameter. The flexibility and whether the fracture of the ribbon occurred were evaluated.

Solidus and liquidus temperatures of the ribbons were obtained by Differential Thermal Analysis (DTA) measurements done with a Setaram Thermal Analyser Setsys 16/18 in an argon atmosphere.

For the identification of the phases formed at ribbons and determination of the crystallinity degree, X-Ray Diffractions (XRD) were performed using a Cu Kα X-ray source in a PANalytical X'Pert Pro MRD diffractometer.

The microstructural studies of the ribbons and brazed joints were performed in the cross section cut by Scanning Electron Microscopy (SEM, S3400 Hitachi) equipped with Energy Dispersive X-ray analysis

Table 2
Ribbons' dimensions of each condition.

	Length		Width (mm)	Thickness (μm)
	Average (mm)	maximum (mm)		
C1	**8.0 ± 3.2**	**15.53**	**1.86 ± 0.16**	**54**
C2	**12.0 ± 5.8**	**23.1**	**0.879 ± 0.20**	**43**
C3	**10.4 ± 3.7**	**17.92**	**1.522 ± 0.17**	**51**
C4	**12.2 ± 4.7**	**21.2**	**1.716 ± 0.14**	**49**
C5	**20.9 ± 15.1**	**52**	**1.747 ± 0.07**	**48**

(EDX). The cross-sections were metallographically prepared using the standard polishing technique [22]. The distribution of each phase that constituted the filler microstructure, in terms of surface area distribution, was performed by a Leica DMR equipped with Leica Image Pro plus software in 5 different areas of each condition.

The possible effect of the brazing thermal cycle on the mechanical properties of the base materials was evaluated by means of Vickers microhardness. Thus, microhardness profiles from CuCrZr side to the tungsten one, across the braze were traced with an MHV-2SHIMADZU equipment. A 100 g load was applied during 15 s and three indentation lines were made per distance. The separation between neighbors indentations was kept longer than three times the residual imprint sizes.

3. Results

3.1. Ribbons characterization

Cu-Ti ribbons fabricated by melt-spinning technique were not fully continuous, resulting in the formation of small ribbons or flakes, depending on the parameters used. The average dimensions for each fabrication condition are shown in Table 2. According to the results, condition C5 has longer filler measurements, which is needed to cover, at least, one rotation of the tubular pipe, which is 50 mm in this case. However, it is expected shorter lengths in the case of DEMO pipes. The maximum length of some ribbons obtained is enough for that purpose. Conditions 1 to 4 did not fulfil this requirement. Regarding the other dimensions of the ribbons, the width of C1, C3, C4, and C5 are similar, in the range of 1.5–1.8 mm but thinner in the case of C2. Finally, all conditions showed similar thickness, around 43–54 μm.

As it is shown in Fig. 2, there is a significant difference in the appearance of ribbons fabricated with different conditions. Ribbons of conditions 1 to 4 have more flake-like geometries, whereas condition 5 showed a more consistent ribbon geometry.

The proposed filler manufacturing process uses high cooling rates, around 10^6 K/s, which hindered diffusion phenomena during the solidification process and gave rise to a more homogenous composition based on a Cu_3Ti and Cu_4Ti phases, according to the X-ray diffraction pattern shown in Fig. 3. Therefore, the cooling rates used in the melt-spinning were not high enough to achieve the formation of an amorphous structure. All conditions showed the formation of both intermetallic compounds, however, condition C5 shows less intensity of the diffraction pattern and the formation of two new diffraction peaks at angles of 44 and 72. The lower intensity could be related to the formation of a semicrystalline structure. These facts could be associated with the lower diameter of the nozzle used in this condition, that reduced the material flow through the nozzle ejected to the wheel producing a more effective cooling process.

Same effect was shown by Tamura et al. [16]. They found that when increased the diameter appeared crystalline structure in $SmFe_9$.

Obtained micrographs using the back scattering electron detector of the ribbon microstructures are shown in the Fig. 4. In all cases, is possible to identify two main phases, which corresponded to those identified in the X-Ray diffraction analysis. The first one is the Cu_3Ti phase, 71Cu-29Ti in at. %, according to the semiquantitative EDS analysis, acted as a matrix phase and the second one is the Cu_4Ti, 77Cu-23Ti in at. % according to the EDS analysis, showed a darker tonality due to the higher titanium content. This last phase appeared as isolated precipitates homogeneously distributed in the Cu_3Ti matrix. The microstructure has changed with respect to previous work, where the filler was obtained by slicing a filler from a Cu-20Ti solidified drop alloy [13]. Although the same phases appeared, the proportion is quite different, being in the actual case Cu_3Ti phase more abundant, which may be associated with the technique studied in this article.

The microstructure comparison among the different tested conditions did not show a great difference. However, the quantification analysis of the phases in the studied surfaces, analyzing at least 5 different zones, showed a decreasing proportion of the Cu_4Ti phase from C1 to C5, as shown in Table 3. This phase is harder and more brittle

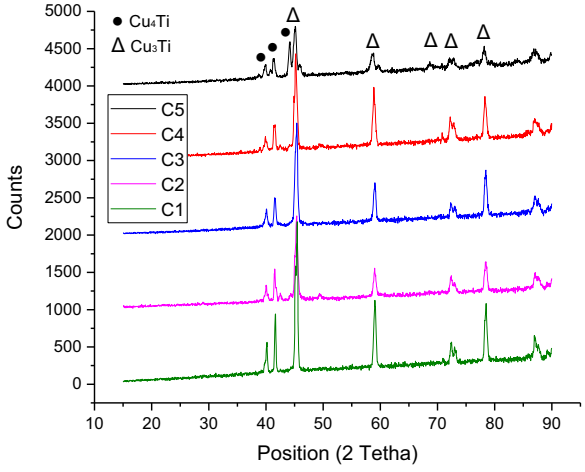

Fig. 3. X-ray diffraction pattern of the ribbons.

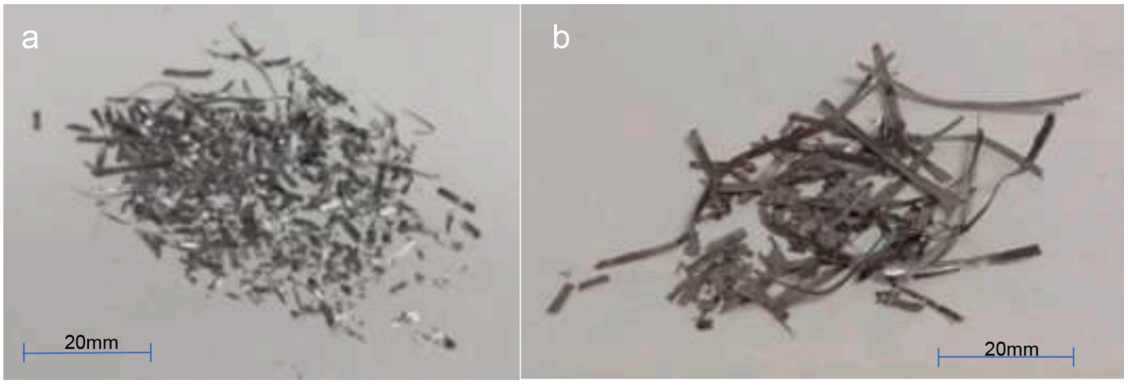

Fig. 2. Image of the fabricated ribbons using (a) C3 and (b) C5 conditions.

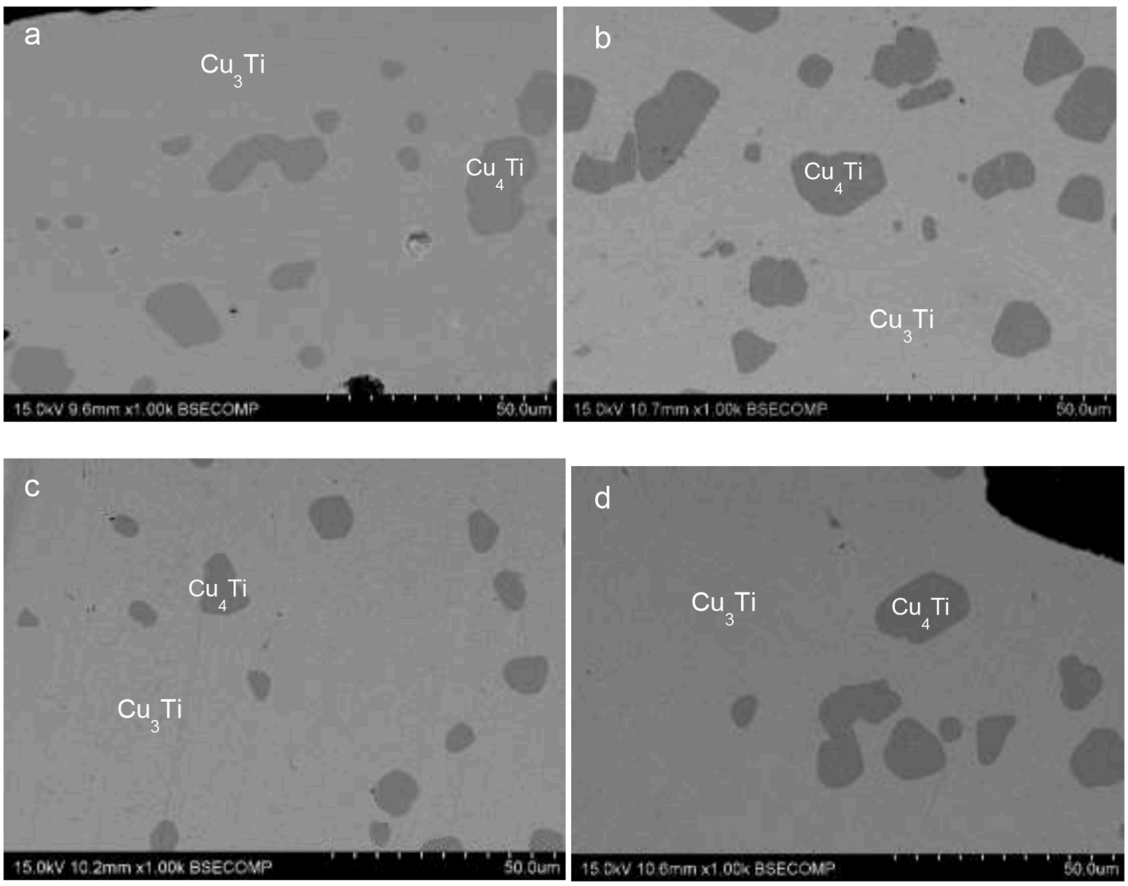

Fig. 4. Cross-section images obtained by SEM of the ribbons microstructure for (a) C2 (b) C3 (c) C4 and (d) C5

Table 3
Phases surface distribution.

Cond	% phase Cu_3Ti	% phase Cu_4Ti
C1	**87,6**	**12,4**
C2	**88**	**11**
C3	**89.5**	**10.5**
C4	**90.25**	**9.75**
C5	**91.4**	**8.6**

compared to the Cu_3Ti phase [23], which increases the brittleness of the ribbon and will be detrimental to the main objective of this work.

In order to determine the flexible and adaption capabilities of the fabricated ribbons, which is necessary for its application in the divertor, flexibility and adaptability tests were carried out using a similar divertor pipe component, as it is shown in Fig. 5a. The results have shown that only conditions 3, 4 and 5 had sufficient flexibility to cover the surface pipe and, only condition 5, had enough length to cover the whole pipe surface. Those properties are achieved by the modification of the microstructure, in which the presence of a higher Cu_4Ti proportion, as it is shown in Table 3, hinders the flexible and adaptability properties. This behavior is associated to the harder and brittle character of Cu_4Ti phase with regard to Cu_3Ti phase [23]. Besides, Cu_4Ti precipitates also acted as a stress concentration point during the application of the force in the adaptability test and, therefore, the increase of theses precipitates produces the premature failure of the filler with respect to microstructures containing lower number of precipitates.

The short length and width of the other conditions made difficult to cover the whole pipe surface and, in some cases, as shown in Table 4, some conditions fracture and did not pass the test (Fig. 5b).

DTA tests were performed to determine the melting range of the fabricating ribbons and the possible effect of the fabrication conditions

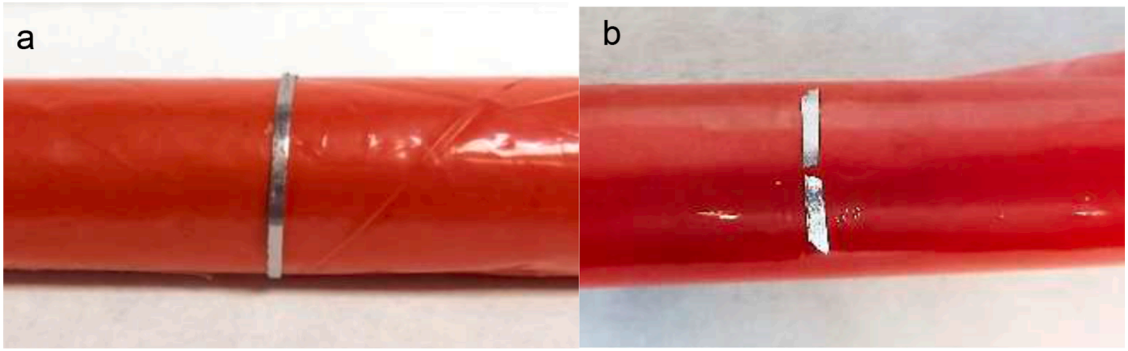

Fig. 5. Top view of (a) C5 and (b) C1 ribbons with crack.

Table 4
Results of adaptability tests.

Cond	Flexibility sufficient to cover surface pipe	Enough length to cover whole pipe
C1	**Yes**	**No**
C2	**Yes**	**No**
C3	**No**	**No**
C4	**No**	**No**
C5	**No**	**Yes**

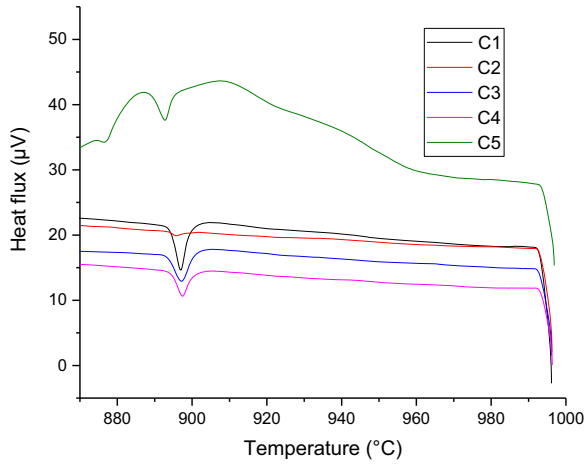

Fig. 6. DTA of the different conditions during heating stage with detail of the melting range.

Table 5
Melting range of different conditions tested.

Cond	T_{sol} (°C)	T_{liq} (°C)
C1	893	900
C2	893	898
C3	892	901
C4	893	901
C5	888	896

used (Fig. 6).

Solidus and liquidus temperatures of the different conditions are presented in Table 5. It can be observed that the melting range of C1 to C4 conditions is quite similar varying from 892 to 893 °C the solidus temperatures and 898–901 °C the liquidus temperature. However, condition 5 melting range shifted to lower temperatures from 888 to 896 °C of solidus and liquidus temperature, respectively. This change can be attributed to a more homogenous composition and microstructure, which can reach more readily the melting composition during heating, whereas in the other cases diffusion must take place to homogenize the composition and melt.

In all cases the obtained melting range is quite small, varying from 5 °C to 9 °C of C2 and C3, respectively. This fact is desirable for the proposed application because implies better flowability and wetting properties of the filler, which ease the filling process of the braze area and gives rise to more continuous joints without pores or nonwetted areas. The reduced melting range is especially important if it is compared with other filler fabrication methods of the same filler composition, where the solidus and melting temperatures were 805 and 909 °C, respectively [13].

3.2. Microstructural characterization of the brazed joints

According to the characterization results obtained in the previous sections, 3 conditions were selected that best optimized the desired properties for its application as filler material in W-CuCrZr joints. These conditions were C3, C4 and C5. All have shown adaptability properties to the pipe surface, present the least presence of brittle phase Cu_4Ti and have dimensions high enough for its manual manipulation and to cover the joint surface area.

The microstructural examination of all conditions showed the consecution of a full metallic continuity, where the presence of cracks or pores was not detected in the brazed area (Fig. 7). The braze width was slightly less than 50 μm in concordance with the thickness of the filler ribbons as fabricated conditions.

The microstructure of the braze using different fillers is similar and is formed by a layer of 80Cu-20Ti in w%, pointed 2 in Fig. 7a–c, according to the EDS analysis, phase in contact with W base material. Above the layer a eutectic-like microstructure is formed constituted by a copper-rich matrix phase and acicular structures of 87Cu-10Ti-2Cr-1Zr (white arrows in Fig. 7a–c).

In all conditions, dark tonality precipitates (pointed 1 in Fig. 7a–c) were also detected with a 60Cu-40Ti in at % composition. All these phases can be observed more in detail in Fig. 8a.

According to the elemental mapping distribution shown in Fig. 8b there was no sign of diffusion or dilution phenomena between tungsten and the braze elements at the interface. The brazing conditions used in this investigation did not activate solid-state diffusion phenomena at the interface. Tungsten, as a refractory material, needs higher temperatures to overcome the activation energy gap [24,25] and activate the diffusion mechanisms. Besides, the solubility of copper in W is almost insistent and, therefore, dilution or diffusion phenomena are not promoted.

To evaluate the thermal affectation and modification of the base materials properties by the application of the brazing process, a microhardness profile was traced from one base material to the other through the braze. The results shown in Fig. 9 indicated that microhardness of W keept constant in the profile and corresponded to the hardness of base material in as-received conditions (440 $HV_{0.1}$) [26]. However, the hardness of the CuCrZr base material decreased with respect to the as-received hardness (120 $HV_{0.1}$) [27]. This fact could be associated to a partial solubilization of the hardening precipitates, grain growth, or recrystallization process at the brazing temperature [28]. These results indicated that, in future works, the application of thermal treatment to

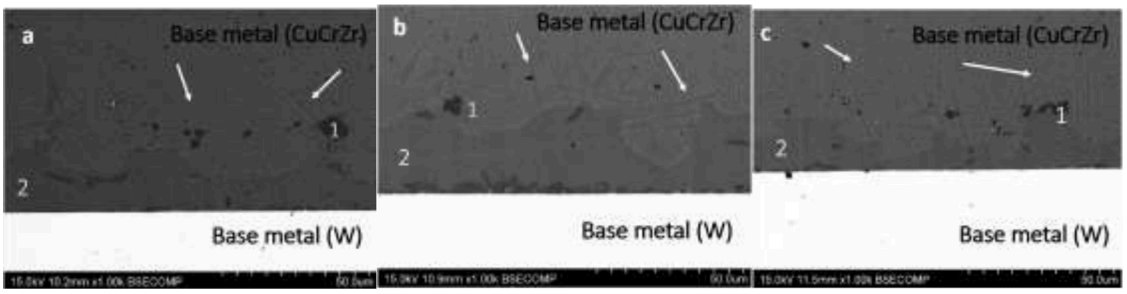

Fig. 7. SEM micrograph of the W-CuCrZr brazed joint at: (a) C3 (b) C4 (c) C5.

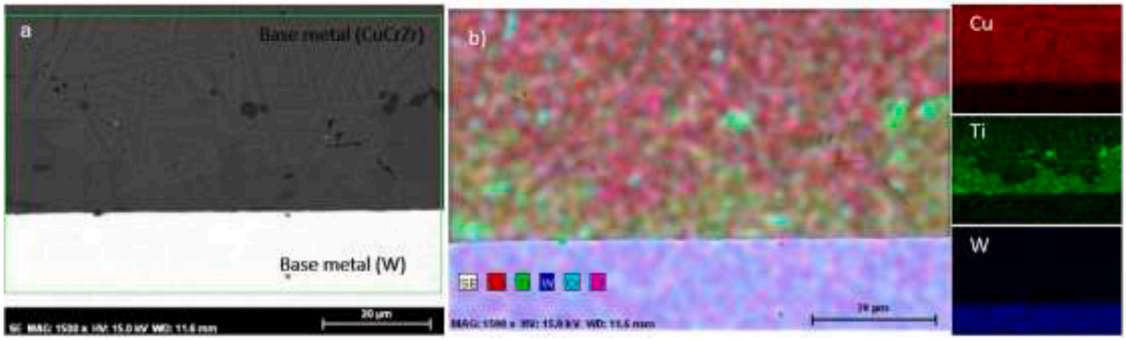

Fig. 8. (a) Details of interface W-CuCrZr (b)Elemental mapping distribution of C5.

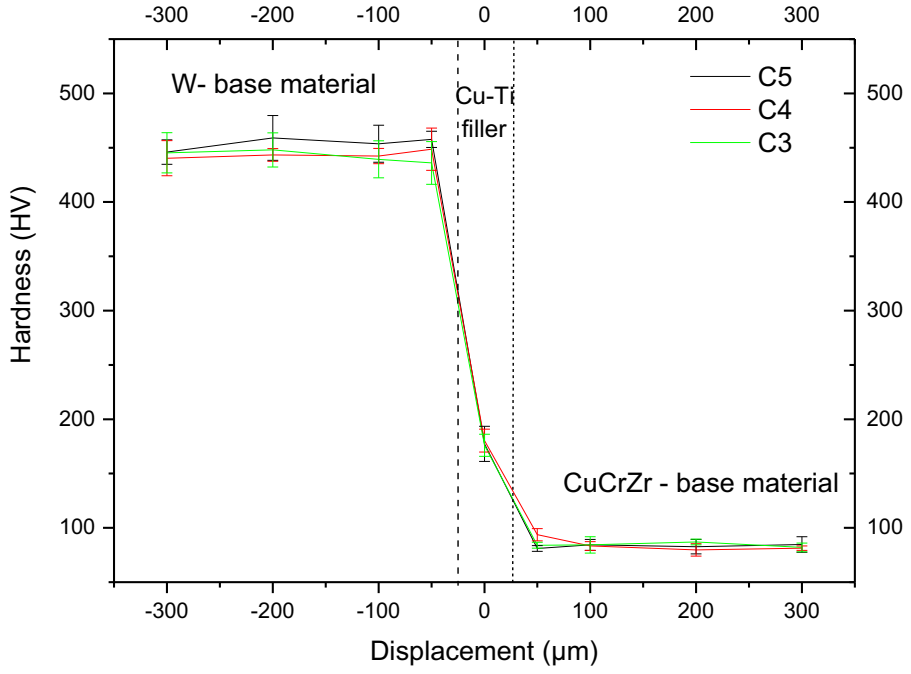

Fig. 9. Microhardness profile of the W-CuCrZr brazed joint across the braze of C3, C4 and C5.

recover the CuCrZr hardness properties should be addressed.

Finally, braze microhardness is characterized by the heterogeneous microstructure previously described, but the mean value is the result of the presence of Cu_3Ti and Cu_4Ti phases, which is higher than the CuCrZr base material due to its intermetallic nature.

4. Conclusion

The use of the melt-spinning technique for filler fabrication did not avoid the formation of a crystalline structure, but it conferred enough flexible capabilities for its adaptions to curved pipes in the divertor or first wall components.

The best manufacturing condition, considering the flexible capabilities and dimensions of the ribbon, had a nozzle diameter of 0.8 mm and a wheel speed of 30 m/s. These conditions allow the fabrication of flexible ribbons of more than 5 cm length, enough to cover the perimeter of the pipe.

Microstructural observation and DTA analysis of the ribbons showed the formation of similar microstructure in all conditions and melting ranges.

Taking into account the previous characterization of ribbons, 3 conditions, a nozzle diameter of 0.8 mm and a wheel speed of 30 m/s, a nozzle diameter of 0.9 mm and a wheel speed of 30 m/s and a nozzle diameter of 0.8 mm and a wheel speed of 35 m/s were selected for its use as a filler in W-CuCrZr joints. All joints showed a high metallic continuity without pores or wetting problems.

The microstructural study revealed that the braze is constituted by a 80Cu-20Ti phase, which forms a layer close to W base material and a eutectic-like microstructure formed by acicular structures of 87Cu-10Ti-2Cr-1Zr and Cu-rich phase. Finally, high Ti content precipitates heterogeneously distributed were detected in the brazing.

Considering the overall results, further investigation should be carried out to achieve the fabrication of larger dimension ribbons. This could be addressed by the addition of amorphization elements in the alloy, which inhibit the crystalline structure formation and, therefore, larger ribbons with flexible capabilities could be obtained.

CRediT authorship contribution statement

I. Izaguirre: Methodology, Validation, Formal analysis, Investigation, Data curation, Writing – original draft, Visualization. **J. de Prado:** Methodology, Validation, Formal analysis, Investigation, Data curation, Writing – original draft, Visualization. **M. Sánchez:** Conceptualization, Formal analysis, Investigation, Resources, Writing – review & editing, Visualization, Supervision, Project administration, Funding acquisition. **D. Salazar:** Methodology, Validation, Formal analysis, Investigation,

Data curation, Writing – original draft, Visualization. **A. Ureña:** Conceptualization, Formal analysis, Investigation, Resources, Writing – review & editing, Visualization, Supervision, Project administration, Funding acquisition.

Declaration of Competing Interest

The authors declare the following financial interests/personal relationships which may be considered as potential competing interests:

Ignacio Izaguirre reports financial support was provided by Rey Juan Carlos University.

Data availability

No data was used for the research described in the article.

Acknowledgments

This work has been carried out within the framework of the EUROfusion Consortium, funded by the European Union via the Euratom Research and Training Programme (Grant Agreement No 101052200 — EUROfusion). Views and opinions expressed are however those of the author(s) only and do not necessarily reflect those of the European Union or the European Commission. Neither the European Union nor the European Commission can be held responsible for them. The authors would also like to acknowledge the Community of Madrid in the framework of the Multiannual Agreement with the Rey Juan Carlos University in line of action 1, "Encouragement of Young Phd student's investigation" Project Ref. M 2168 Acronym DARUCEF. D. Salazar acknowledge support from the EU Horizon 2020 research and innovation programme under Grant Agreement No. 862617 – Multi-Fun.

References

[1] T.R. Barrett, et al., Progress in the engineering design and assessment of the European DEMO first wall and divertor plasma facing components, Fusion Eng. Des. 109–111 (2016) 917–924, https://doi.org/10.1016/j.fusengdes.2016.01.052.

[2] G. Federici, et al., Overview of the design approach and prioritization of R&D activities towards an EU DEMO, Fusion Eng. Des. 109–111 (2016) (2016) 1464–1474, https://doi.org/10.1016/j.fusengdes.2015.11.050.

[3] P. Gavila, et al., Status of the ITER Divertor IVT procurement, Fusion Eng. Des. 160 (2020), 111973, https://doi.org/10.1016/j.fusengdes.2020.111973 no. September.

[4] P. Liu, X. Qian, X. Mao, W. Song, X. Peng, Study on creep-fatigue of heat sink in W/CuCrZr divertor target based on a new approach to creep life, Nucl. Mater. Energy 25 (2020), 100846, https://doi.org/10.1016/j.nme.2020.100846.

[5] Y. Chen, et al., High-strength diffusion bonding of oxide-dispersion-strengthened tungsten and CuCrZr alloy through surface nano-activation and Cu plating, J. Mater. Sci. Technol. 92 (2021) 186–194, https://doi.org/10.1016/j.jmst.2021.03.040.

[6] Y. Li, C. Chen, R. Yi, Y. Ouyang, Review: special brazing and soldering, J. Manuf. Process. 60 (2020) 608–635, https://doi.org/10.1016/j.jmapro.2020.10.049, no. October.

[7] J. de Prado, M. Sánchez, A. Ureña, Improvements in W-Eurofer first wall brazed joint using alloyed powders fillers, Fusion Eng. Des. 124 (2017) 1082–1085, https://doi.org/10.1016/j.fusengdes.2017.03.126.

[8] N. Mou, et al., Manufacturing and high heat flux testing of flat-type W/Cu/CuCrZr mock-up by HIP assisted brazing process, Fusion Eng. Des. 169 (2021), 112670, https://doi.org/10.1016/j.fusengdes.2021.112670 no. February.

[9] K.P. Singh, S.S. Khirwadkar, K. Bhope, N. Patel, P. Mokaria, Feasibility study on joining of multi-layered W/Cu-CuCrZr-SS316L-SS316L materials using vacuum brazing, Fusion Eng. Des. 127 (2018) 73–82, https://doi.org/10.1016/j.fusengdes.2017.12.027, no. July 2017.

[10] L. Peng, Y. Mao, Y. Zhang, L. Xi, Q. Deng, G. Wang, Microstructural and mechanical characterizations of W/CuCrZr and W/steel joints brazed with Cu-22TiH2 filler, J. Mater. Process. Technol. 254 (2018) 346–352, https://doi.org/10.1016/j.jmatprotec.2017.11.056, no. August 2017.

[11] J. Yang, Y. Xu, S. Zhang, M. Zhang, Joining of Mn-Cu alloy and 430 stainless steel using Cu-based filler by SIMA-imitated brazing process, Mater. Lett. 253 (2019) 401–404, https://doi.org/10.1016/j.matlet.2019.06.098.

[12] S. Buhl, C. Leinenbach, R. Spolenak, K. Wegener, Microstructure, residual stresses and shear strength of diamond-steel-joints brazed with a Cu-Sn-based active filler alloy, Int. J. Refract. Met. Hard Mater. 30 (1) (2012) 16–24, https://doi.org/10.1016/j.ijrmhm.2011.06.006.

[13] J. de Prado, M. Sánchez, A. Ureña, Evaluation of mechanically alloyed Cu-based powders as filler alloy for brazing tungsten to a reduced activation ferritic-martensitic steel, J. Nucl. Mater. 490 (Jul. 2017) 188–196, https://doi.org/10.1016/j.jnucmat.2017.04.033.

[14] J. de Prado, M. Sánchez, D. Swan, A. Ureña, Microstructural and mechanical characterization of W-cucrzr joints brazed with Cu-Ti filler alloy, Metals (Basel) 11 (2) (2021) 1–9, https://doi.org/10.3390/met11020202.

[15] S.A. Rogachev, O. Politano, F. Baras, A.S. Rogachev, Explosive crystallization in amorphous CuTi thin films: a molecular dynamics study, J. Non Cryst. Solids 505 (2019) 202–210, https://doi.org/10.1016/j.jnoncrysol.2018.10.040, no. August 2018.

[16] T. Tamura, M. Li, Influencing factors on the amorphous phase formation in Fe–7.7 at% Sm alloys solidified by high-speed melt spinning, J. Alloy. Compd. 826 (2020), 154010, https://doi.org/10.1016/j.jallcom.2020.154010.

[17] D. Salazar, A. Martin-Cid, R. Madugundo, J.S. Garitaonandia, J.M. Barandiaran, G. C. Hadjipanayis, Effect of Nb and Cu on the crystallization behavior of under-stoichiometric Nd-Fe-B alloys, J. Phys. D Appl. Phys. 50 (2017), 015305.

[18] M. Bouhbou, et al., Magnetic, magnetocaloric and critical exponent properties of amorphous Fe67Y33 ribbons prepared by melt-spinning technique, Phys. Stat. Mech. Appl. 534 (2019), https://doi.org/10.1016/j.physa.2019.122088.

[19] J. de Prado, M. Sánchez, A. Ureña, Wettability study of a Cu-Ti alloy on tungsten and EUROFER substrates for brazing components of DEMO fusion reactor, Mater. Des. 99 (2016) 93–101, https://doi.org/10.1016/j.matdes.2016.03.054.

[20] D. Salazar-Jaramillo, et al., Chapter Six - Lightweight, multifunctional materials based on magnetic shape memory alloys, in: P. Costa, C.M. Costa, S.B.T.-A.L.M. M. Lanceros-Mendez (Eds.), Woodhead Publishing in Materials, Woodhead Publishing, 2021, pp. 187–237.

[21] G. Geng, D. Wang, W. Zhang, L. Liu, A.M. Laptev, Fabrication of Cu–Ni–Si alloy by melt spinning and its mechanical and electrical properties, Mater. Sci. Eng. A 776 (2020), 138979, https://doi.org/10.1016/j.msea.2020.138979 no. November 2019.

[22] American Society for Testing and Materials, "Standard Guide for Preparation of Metallographic Specimens 1," vol. 03, no. July, 2001.

[23] J. de Prado, M. Roldán, M. Sánchez, V. Bonache, J. Rams, A. Ureña, Interfacial characterization by TEM and nanoindentation of W-Eurofer brazed joints for the first wall component of the DEMO fusion reactor, Mater. Charact. 142 (2018) 162–169, https://doi.org/10.1016/j.matchar.2018.05.035, no. May.

[24] E. Tejado, et al., Thermomechanical characterisation of W-Eurofer 97 brazed joints, J. Nucl. Mater. 542 (2020), 152504, https://doi.org/10.1016/j.jnucmat.2020.152504.

[25] J. de Prado, M. Sánchez, A. Ruiz, A. Ureña, Effect of brazing temperature, filler thickness and post brazing heat treatment on the microstructure and mechanical properties of W-Eurofer joints brazed with Cu interlayers, J. Nucl. Mater. 533 (May 2020), 152117, https://doi.org/10.1016/j.jnucmat.2020.152117.

[26] J. Aldazabal, et al., A comparison of the structure and mechanical properties of commercially pure tungsten rolled plates for the target of the European spallation source, Int. J. Refract. Met. Hard Mater. 70 (2018) 45–55, https://doi.org/10.1016/j.ijrmhm.2017.09.006, no. September 2017.

[27] S. Mao, D.Z. Zhang, Z. Ren, G. Fu, X. Ma, Effects of process parameters on interfacial characterization and mechanical properties of 316L/CuCrZr functionally graded material by selective laser melting, J. Alloy. Compd. 899 (2022), 163256, https://doi.org/10.1016/j.jallcom.2021.163256.

[28] B. Zhang, Z.G. Zhang, W. Li, Effects of thermo-mechanical treatment on microstructure and properties of Cu-Cr-Zr alloys, Phys. Procedia 50 (2013) 55–60, https://doi.org/10.1016/j.phpro.2013.11.011. October 2012.